Overland Water Flow and Solute Transport: Model Development and Field-Data Analysis

Fariborz Abbasi[1]; Jirka Simunek[2]; M. Th. van Genuchten[3]; Jan Feyen[4]; Floyd J. Adamsen[5]; Douglas J. Hunsaker[6]; Theodore S. Strelkoff[7]; and Peter Shouse[8]

Abstract: The application of plant nutrients with irrigation water is an efficient and cost-effective method for fertilizer application to enhance crop production and reduce or eliminate potential environmental problems related to conventional application methods. In this study, a combined overland water flow and solute transport model for analysis and management of surface fertigation/chemigation is presented. Water flow is predicted with the well-known Saint-Venant's equations using a control volume of moving cells, while solute transport is modeled with the advection-dispersion equation. The 1D transport equation was solved using a Crank-Nicholson finite-difference scheme. Four, large-scale, field experiments were conducted on blocked-end and free draining furrows to calibrate and verify the proposed model. The results showed that application of solute during the entire irrigation event, or during the second half of the irrigation for blocked end conditions with appropriate inflow rates, produced higher solute uniformity than application of solute during the first half of the irrigation event. Measured fertilizer distribution uniformity of the low quarter ranged from 21 to 76% while fertilizer distribution uniformity of the low half values varied between 62 to 87%. The model was subsequently applied to the experimental data; results showed good agreement with all field data. Water balance errors for the different experiments varied from 0.004 to 1.8%, whereas fertilizer mass balance errors ranged from 1.2 to 3.6%. A sensitivity analysis was also performed to assess the effects of longitudinal dispersivity parameter on overland solute concentrations. A value of 10 cm for dispersivity provided a reasonable fit to the experimental data.

DOI: 10.1061/(ASCE)0733-9437(2003)129:2(71)

CE Database subject headings: Overland flow; Furrow irrigation; Dispersion; Fertilization; Data analysis.

Introduction

Fertilizers are widely applied to agricultural fields using surface fertigation, i.e., application of fertilizers with irrigation water. However, there are still no adequate guidelines for the proper design and management of surface fertigation. The method has certain advantages as compared to conventional application methods, such as reduced energy, labor, soil compaction, and machinery costs. Moreover, it allows growers to apply nutrients in small amounts throughout the season in response to crop needs without the possibility of crop damage or soil compaction caused by mechanized application methods. Concerns about the use of surface fertigation stem from the alleged low uniformity and efficiency of surface irrigation systems. Treadgill (1985) conducted a chemigation survey in the United States and found that while 61% of microirrigation and 43% of sprinkler irrigation systems used chemigation, only 3.5% of the surface irrigation systems utilized this technique. Likely reasons for the limited use found for surface fertigation were the typically low uniformity of surface irrigation systems and fertilizer losses due to runoff (Treadgill et al. 1990). However, more recent findings by Hanson et al. (1995) on 959 irrigation fields in California showed that the uniformity of border and furrow irrigation was generally higher than that for all other irrigation systems in the area. These findings indicate that further studies on surface fertigation are needed.

Jaynes et al. (1992) conducted a fertigation experiment and compared the leaching behavior of two conservative mobile tracers. They studied the fate of Br applied in the irrigation water and o-triflouromethyl benzoic acid sprayed on the soil surface before irrigation. Their results implied that application of fertilizers in irrigation water applied in level basins could potentially increase deep leaching of agricultural chemicals. Earlier studies further indicated rapid leaching along preferential flow paths when chemicals were applied with the irrigation water (Bowman and Rice 1986; Jaynes et al. 1988). Preferential flow was also ob-

[1]Institute for Land and Water Management, Katholieke Universiteit Leuven, Belgium, Vital Decosterstraat 102, 3000-Leuven, Belgium. E-mail: FRABBASI@hotmail.com

[2]George E. Brown Jr. Salinity Laboratory, USDA-ARS, 450 West Big Springs Dr., Riverside, CA 92507. E-mail: JSIMUNEK@ussl.ars.usda.gov

[3]George E. Brown Jr. Salinity Laboratory, USDA-ARS, 450 West Big Springs Dr., Riverside, CA 92507. E-mail: RVANG@ussl.ars.usda.gov

[4]Institute for Land and Water Management, Katholieke Universiteit Leuven, Belgium, Vital Decosterstraat 102, 3000-Leuven, Belgium. E-mail: JAN.FEYEN@agr.kuleuven.ac.be

[5]U.S. Water Conservation Laboratory, USDA-ARS, 4331 East Broadway Rd., Phoenix, AZ 85040. E-mail: FADAMSEN@uswcl.ars.ag.gov

[6]U.S. Water Conservation Laboratory, USDA-ARS, 4331 East Broadway Rd., Phoenix, AZ 85040. E-mail: DHUNSAKER@uswcl.ars.ag.gov

[7]U.S. Water Conservation Laboratory, USDA-ARS, 4331 East Broadway Rd., Phoenix, AZ 85040. E-mail: FSTRELKOFF@uswcl.ars.ag.gov

[8]George E. Brown Jr. Salinity Laboratory, USDA-ARS, 450 West Big Springs Dr., Riverside, CA 92507. E-mail: PSHOUSE@ussl.ars.usda.gov

Note. Discussion open until September 1, 2003. Separate discussions must be submitted for individual papers. To extend the closing date by one month, a written request must be filed with the ASCE Managing Editor. The manuscript for this paper was submitted for review and possible publication on October 12, 2001; approved on July 3, 2002. This paper is part of the ***Journal of Irrigation and Drainage Engineering***, Vol. 129, No. 2, April 1, 2003. ©ASCE, ISSN 0733-9437/2003/2-71–81/$18.00.

Table 1. Infiltration and Roughness Parameters, Field and Solute Properties, Furrow Section and Geometry Parameters as the Input Values during Model Performance for Different Field Experiments

	Experiment			
Parameter	100%	First half	Second half	Free draining
Field length, L (m)	115	115	115	115
Furrow spacing, W (m)	1	1	1	1
Field slope, S_o ($m \cdot m^{-1}$)	0.0001	0.0001	0.0001	0.0001
Hydraulic section parameters[a]				
ρ_1 ($m^{3.33-2\rho_2}$)	0.326	0.326	0.326	0.326
ρ_2(-)	2.789	2.789	2.789	2.789
Furrow geometry parameters[b]				
σ_1 ($m^{1/2\sigma_2}$)	0.871	0.871	0.871	0.871
σ_2(-)	0.635	0.635	0.635	0.635
Infiltration parameters				
a(-)	0.75	0.75	0.75	0.78
k ($m^3 \cdot min^{-a} \cdot m^{-1}$)[c]	0.00209	0.00218	0.00288	0.00212
c ($m^3 \cdot m^{-1}$)[c]	0.006	0.006	0.001	0.006
Manning, n ($m^{1/6}$)	0.066	0.066	0.081	0.071
Time of cut-off, T_{co} (min)	140	140	140	275
Inflow rate, Q_o ($L \cdot s^{-1}$)	1.29	1.32	1.28	1.07
Input solute concentration, C_0, (g $Br \cdot L^{-1}$)	2.36	2.79	5.35	6.30
Solute application time, T_f, (min)	140	70	70	275
Dispersivity, D_l, (cm)	10	10	10	10

[a]Furrow section parameters for $A^2R^{4/3}=\rho_1 A^{\rho_2}$.

[b]Furrow geometry parameters for $y=\sigma_1 A^{\sigma_2}$.

[c]Expressed in terms of k ($m \cdot min^{-a}$) and c (m) for 100%, FH, and SH experiments. The EVALUE uses the procedure reported by Strelkoff and Clemmens (2000) to convert the values.

served when tracers were applied to the soil by conventional methods before irrigation events (Rice et al. 1986). Boldt et al. (1994) presented a numerical model for surface fertigation management in surged irrigation of furrows. The writers applied the model to hypothetical conditions for various soils, infiltration, and furrow inflow rates in order to develop optimum fertigation management strategies. The simulation results showed that to obtain proper fertigation efficiency on coarse-textured soils, fertigation could be applied during any or all parts of a surge cycle but should be carried out during all cycles. Moreover, fertigation applications on medium- and fine-textured (low permeability) soils should be made during the entire surge cycle and should be applied either during the entire irrigation event or only during advance surges.

Playan and Faci (1997) evaluated the uniformity of surface fertigation by conducting a series of field experiments on blocked-end borders. They also developed a fertigation model based on the 1D pure advection equation to simulate the experimental data. Results revealed that the fertilizer distribution uniformity of the low half (DU_{LH}) ranged from 3 to 52%, while the water DU_{LH} ranged from 64 to 97%. The best fertigation uniformity was achieved by applying a constant rate during the entire irrigation event. By contrast, a short-duration fertilizer application produced relatively low uniformity. Garcia-Navarro et al. (2000) investigated the effects of the dispersion coefficient on overland solute concentration by executing several experiments on an impervious border. The results exhibited a constant value of 0.075 m^2/s for the indicated parameter. A comparison between numerical results based on the advection-dispersion equation (Garcia-Navarro et al. 2000) and a pure advection model (Playan and Faci 1997) showed that the advection-dispersion model better estimated the observed solute uniformity in the border experiments.

The main objective of this paper is to present a combined model of overland water flow and solute transport for assessing and managing surface fertigation. Results of several field experiments on both blocked-end and free-draining furrows involving surface chemigation are presented, and the data are used to calibrate and verify the model. Uniformity of the applied solute pulse and the effect of longitudinal dispersivity on overland solute concentrations were also evaluated.

Model System Definition

The system presented in this paper combines an overland water flow and solute transport model and applies it to furrows/borders. The integrated model numerically solves the 1D dispersion-advection and simplified form of the Saint-Venant's (Chow 1959) equations as the governing equations in a decoupled fashion. In spite of 2D water flow and solute transport in and below furrows, the authors believe that a simple 1D model can provide plenty of useful information without requiring as many input parameters as need for conducting a 2D analysis. Assuming 1D water flow and solute movement in overland studies, such as furrows, is not too problematic because of the inherent small confined flow areas in furrows. In fact, overland water and solute transport analysis in furrows, because of indicated reason above, could be closer to 1D rather than wide borders and rivers in particular.

The model is applied to evaluate several alternative fertigation practices used in free-draining and blocked-end furrows. It uses geometry of the furrow, infiltration, roughness, flow, and solute properties listed in Table 1 as the input parameters for each furrow and as output, the model predicts overland solute concentrations, flow rates/velocities, flow areas/depths, advance-recession trajectories, and water and solute losses through runoff at the end

of furrow in case of free drainage. Furthermore, the quality of the irrigation and fertigation event is evaluated using the distribution uniformity of the low quarter (DU_{LQ}) and low half (DU_{LH}) indices (Merriam and Keller 1978). As indicated earlier, the developed model is mainly an overland model and cannot provide so much subsurface information such as distribution of infiltrated water and solute. The model just provides water and fertilizer infiltrated at the surface using simple empirical infiltration models (Kostiakov, Kostiakov-Lewis, Philip, and modified Kostiakov branch function) at any desired station along the monitored furrows/borders, which in turn from those results quality of the irrigation and fertigation can be evaluated using distribution uniformity indices. The model also provides total values of water and solute infiltrated throughout the monitored furrows/borders. Initial and boundary conditions required for the solution of the flow equations are well described in relevant references (Abbasi et al. 1999). Details about the proposed model are discussed in the following sections.

Governing Equations

Hydrodynamic dispersion and advection are the two most important processes governing solute transport during surface fertigation. Using the hypotheses of Holley (1971) that differential convective transport and turbulent diffusion processes may be combined in gradient diffusion terms, the 1D cross-sectional average dispersion equation for surface fertigation is as follows (Cunge et al. 1980):

$$\frac{\partial(AC)}{\partial t}+\frac{\partial(AUC)}{\partial x}=\frac{\partial}{\partial x}\left(AK_x\frac{\partial C}{\partial x}\right) \tag{1}$$

where C ($kg\cdot m^{-3}$) and U ($m\cdot s^{-1}$)=cross-sectional average concentration and velocity, respectively; A (m^2)=flow area; K_x ($m^2\cdot s^{-1}$)=dispersion coefficient; and t (s) and x (m)=time and space, respectively. The dispersion coefficient K_x incorporates both dispersion due to differential advection and turbulent diffusion (Cunge et al. 1980). The dispersion coefficient for transport in soils can generally be described by (Bear 1972)

$$\theta K_x=D_l q_x+\theta D_d\tau_0 \tag{2}$$

where θ=volumetric water content ($cm^3\cdot cm^{-3}$); τ_0=tortuosity factor (-); q_x=flux density at location x ($m\cdot s^{-1}$); D_l=longitudinal dispersivity (m); and D_d=molecular diffusion in free water ($m^2\cdot s^{-1}$). Eq. (2) for overland flow, letting $\theta=1$ and $\tau=1$, simplifies to

$$K_x=D_l U_x+D_d \tag{3}$$

where U_x=overland flow velocity at location x ($m\cdot s^{-1}$).

The solution of the advection-dispersion Eq. (1) requires a solution for the Saint-Venant's (Chow 1959) equations governing water flow. The Saint-Venant's and advection-dispersion equations are solved sequentially at each time step. The simplified Saint-Venant's equations, without inertia terms, are as follows:

$$\frac{\partial A}{\partial t}+\frac{\partial Q}{\partial x}+\frac{\partial Z}{\partial t}=0 \tag{4}$$

and

$$\frac{\partial y}{\partial x}=S_0-S_f \tag{5}$$

where Q=flow rate ($m^3\cdot s^{-1}$); y=flow depth (m); S_0=field slope ($m\cdot m^{-1}$); S_f=hydraulic resistance slope ($m\cdot m^{-1}$); and Z=infiltrated water volume per unit length of the field ($m^3\cdot m^{-1}$). The infiltrated water volume was formulated using the modified Kostiakov branch function (Strelkoff et al. 1999)

$$Z=c+k\tau^a;\quad \tau\leqslant\tau_B$$
$$Z=c_B+b\tau;\quad \tau>\tau_B \tag{6}$$

where τ=infiltration opportunity time (min); τ_B=inundation time (min); and c ($m^3\cdot m^{-1}$), c_B ($m^3\cdot m^{-1}$), a (-), k ($m^2\cdot min^{-a}$), and b ($m^2\cdot min^{-a}$)=empirical constants.

The above flow and transport models suffer from several limitations. One limitation is the inherent Fickian approximation in Eq. (1), which is only valid at large distances from the injection point. The Fickian approximation is valid for rivers with large flow cross-sectional areas, rather than for furrows with relatively small flow rates and areas. A second limitation deals with the hypothesis behind the Saint-Venant's equations that continuity and momentum equations are vertically averaged (Playan and Faci 1997).

Solution Techniques

Water Flow Model

The governing equations for water flow [Eqs. (4) and (5)] were solved in the form of a zero-inertia model, ZIMOD (Abbasi et al. 1999) using a control volume of moving cells and then linearized by means of a Newton-Raphson algorithm. The resulting algebraic equations were solved iteratively by applying the Gaussian elimination technique. The ZIMOD can simulate all phases of both border and furrow irrigation systems with either free draining or blocked-end conditions. The model was verified and validated against several field experiments under different irrigation methods, soil infiltration properties, field lengths, and slopes. More details about the ZIMOD are given by Abbasi et al. (1999, 2003).

Fertigation Model

Numerical solutions of the 1D advection-diffusion equation, subject to appropriate initial and boundary conditions, under conditions of overland flow require a great deal of care because of the dominance of the advection term in Eq. (1). Most finite-difference approaches for calculating the convection term of Eq. (1) are plagued by problems of numerical oscillations and/or artificial or numerical dispersion, which is sometimes larger than the actual physical dispersion. A Crank-Nicholson finite difference scheme with a small truncation error of the order of $[(\Delta x)^2+(\Delta t)^2]$ was used to numerically solve Eq. (1). The following discretization was used:

$$\frac{(AC)_i^{n+1}-(AC)_i^n}{\Delta t}+f\frac{(AUC)_i^{n+1}-(AUC)_{i-1}^{n+1}}{x_i-x_{i-1}}$$
$$+(1-f)\frac{(AUC)_i^n-(AUC)_{i-1}^n}{x_i-x_{i-1}}$$
$$=f\left[\frac{Kx_{i+1/2}^{n+1}A_{i+1/2}^{n+1}\left.\frac{\partial C}{\partial x}\right|_{i+1/2}^{n+1}-Kx_{i-1/2}^{n+1}A_{i-1/2}^{n+1}\left.\frac{\partial C}{\partial x}\right|_{i-1/2}^{n+1}}{x_{i+1/2}-x_{i-1/2}}\right]$$
$$+(1-f)\left[\frac{Kx_{i+1/2}^{n}A_{i+1/2}^{n}\left.\frac{\partial C}{\partial x}\right|_{i+1/2}^{n}-Kx_{i-1/2}^{n}A_{i-1/2}^{n}\left.\frac{\partial C}{\partial x}\right|_{i-1/2}^{n}}{x_{i+1/2}-x_{i-1/2}}\right] \tag{7}$$

where subscript i and superscript n denote the space and time intervals, respectively; and f=real constant within the interval $0 \leq f \leq 1$. When $f=0$ the solution system is explicit and when $f=1$ the system is implicit. For implicit schemes, which are unconditionally stable under most circumstances, the resulting set of equations must be solved simultaneously. In implicit approaches, if f is large enough, the value of the time increment, Δt, becomes less dependent on the space increments, Δx. These schemes generally provide a numerical method that is computationally very efficient.

Discretization of the remaining terms on the right hand side of Eq. (7) and rearrangement leads to the following linear algebraic equation at each time step:

$$(a_i)C_{i-1}^{n+1}+(d_i)C_i^{n+1}+(b_i)C_{i+1}^{n+1}=e_i \tag{8}$$

where

$$a_i=-\frac{f\Delta t(AU)_{i-1}^{n+1}}{x_i-x_{i-1}}-\frac{2f\Delta tKx_{i-1/2}^{n+1}A_{i-1/2}^{n+1}}{(x_{i+1}-x_{i-1})(x_i-x_{i-1})} \tag{9}$$

$$b_i=-\frac{2f\Delta tKx_{i+1/2}^{n+1}A_{i+1/2}^{n+1}}{(x_{i+1}-x_{i-1})(x_{i+1}-x_i)} \tag{10}$$

$$d_i=A_i^{n+1}+\frac{f\Delta t(AU)_i^{n+1}}{x_i-x_{i-1}}+\frac{2f\Delta tKx_{i+1/2}^{n+1}A_{i+1/2}^{n+1}}{(x_{i+1}-x_{i-1})(x_{i+1}-x_i)}+\frac{2f\Delta tKx_{i-1/2}^{n+1}A_{i-1/2}^{n+1}}{(x_{i+1}-x_{i-1})(x_i-x_{i-1})} \tag{11}$$

$$e_i=(AC)_i^n-\frac{(1-f)\Delta t}{x_i-x_{i-1}}[(AUC)_i^n-(AUC)_{i-1}^n]+\frac{2(1-f)\Delta t}{(x_{i+1}-x_{i-1})}\left[Kx_{i+1/2}^nA_{i+1/2}^n\frac{C_{i+1}^n-C_i^n}{x_{i+1}-x_i}-Kx_{i-1/2}^nA_{i-1/2}^n\frac{C_i^n-C_{i-1}^n}{x_i-x_{i-1}}\right] \tag{12}$$

Eq. (8) is a tridiagonal system of linear equations that can be solved efficiently using the Thomas algorithm (Thomas 1949). While the solution of Eq. (8) depends on a numerical solution of the water flow equations, the reverse is not true, because flow equations can be solved independently of the advection-diffusion equation. Hence, the two models can be formulated and solved in a sequential but uncoupled fashion.

The solution of Eq. (8) requires that the flow area and the cross-sectional average velocities for each node be obtained first from the solution of the flow equations. The surface irrigation model itself does not provide flow velocities directly; those must be derived by dividing the flow rates, Q_i, by the flow areas, A_i, for each node, e.g., $U_i=Q_i/A_i$. Therefore, the procedure applied at each time step is to first solve the flow equations and then, given the flow areas and velocities, to solve the advection-dispersion equation to obtain overland solute concentrations in the irrigation water at different locations along the field.

Boundary and Initial Conditions

Eq. (8) is a linear parabolic partial differential equation that requires one upstream and one downstream boundary condition, as well as knowledge of the initial state. The upstream boundary condition is the known applied solute concentration as a function of time. The downstream boundary condition is generally a zero concentration gradient. A zero value was used as the initial condition along the entire furrows.

Time and Space Discretizations

Numerical solutions of Eq. (8) often exhibit oscillatory behavior and/or artificial numerical dispersion near relatively sharp concentration fronts. These problems can be especially serious when convection dominates dispersion such as during overland flow. Undesired oscillations can be limited or avoided by selecting appropriate space and time discretizations. Two dimensionless numbers, the Peclet and Courant numbers, may be used to characterize the space and time discretizations for the fertigation model. The Peclet number is ratio of the convective and dispersive transport terms relative to coarseness of the spatial grid size as follows:

$$P_e=\frac{U_x\Delta x}{K_x} \tag{13}$$

To achieve acceptable numerical results, the spatial discretization must be kept relatively fine to maintain a low Peclet number. Numerical oscillations can be virtually eliminated when the local Peclet numbers do not exceed about 5, while relatively small but acceptable oscillations can be obtained with local Peclet number as high as 10 (Huyakorn and Pinder 1983).

A second dimensionless number, the Courant number, C_r, characterizes the relative extent of numerical oscillations. The Courant number is closely associated with the time discretization as follows:

$$C_r=\frac{U_x\Delta t}{\Delta x} \tag{14}$$

In order to achieve stable oscillation-free solutions, the Courant number generally must remain less than about one. The maximum time and space discretizations for the fertigation model are calculated using Eqs. (13) and (14) and considering the Peclet and Courant numbers equal to 10 and 1, respectively. A constant value of U_x at inlet was used in calculating time and space increments.

The solution of the water flow equations is implemented with variable space increments, Δx_i, to enable special conditions associated with the water flow regime. Δx_i is determined simultaneously with the flow areas and flow rates at each time step during the advance phase of irrigation. Unlike the surface irrigation model, the fertigation model is executed with constant Δx to facilitate adherence to the stability criteria. The nodal values of the flow areas, A_i, and the velocities, U_i, obtained from the numerical solution of the surface irrigation model, are associated with the variable grid system involving different space intervals, Δx_i. Hence, they must be interpolated to constant space intervals, Δx to be used in numerical solutions of Eq. (8). Solutions of Eq. (8) at each time step are subsequently obtained at constant Δx to simulate overland solute concentrations along the field.

Infiltrated Solute Mass

The mass of solute F_z (kg/m) infiltrated through the soil surface into the soil between two consecutive time steps can be estimated using the overland solute concentrations and infiltrated amount of water as

$$F_z=\sum_{i=1}^{n}(Z_i^{t+\Delta t}-Z_i^t)\times\frac{(C_i^{t+\Delta t}+C_i^t)}{2} \tag{15}$$

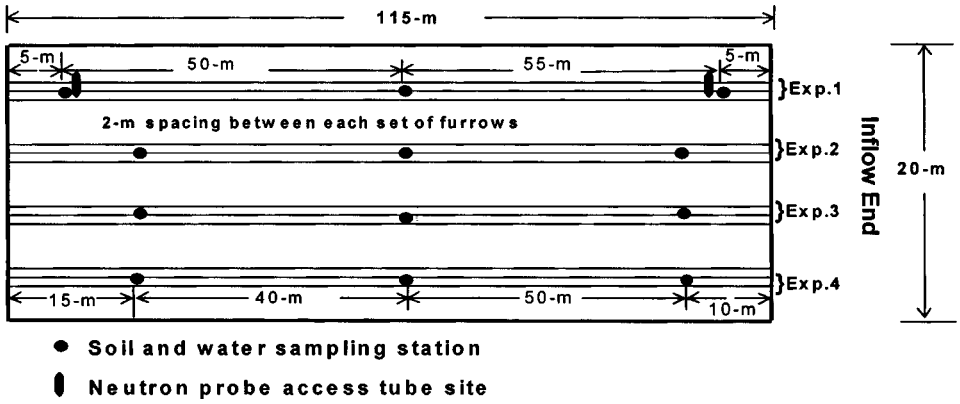

Fig. 1. Plane view of the furrow irrigation field experiments at Maricopa Agricultural Center near Phoenix, Ariz. (axes are not to scale)

where n=number of nodes along the length of the field; and Z_i^t=volume of infiltrated water per unit length at node i and time level t.

The mass of fertilizer losses due to runoff from the field downstream, F_R (kg), can be estimated using outflow rates and overland water concentrations as follows:

$$F_R=\frac{(Q_R^{t+\Delta t}+Q_R^t)}{2}\times\frac{(C_i^{t+\Delta t}+C_i^t)}{2}\times\Delta t \tag{16}$$

where Q_R=outflow rate ($m^3\cdot s^{-1}$) at the end of field.

Irrigation and surface fertigation uniformities were evaluated using the distribution uniformity of the low quarter (DU_{LQ}) and low half (DU_{LH}) as described by Merriam and Keller (1978) for the infiltrated irrigation depth.

Field Experiments

Four, large-scale, furrow experiments, one under free draining and three under blocked-end conditions, were conducted at the Maricopa Agricultural Center (MAC), Maricopa, Phoenix, Ariz. in 2001 to calibrate and validate the developed model. The experiments were carried out on 115-m furrows spaced 1 m apart. Each experiment included three irrigated furrows, one monitored, nonwheel furrow in the middle, and two nonmonitored wheel furrows, one at each side. A plane view of the experiments is shown in Fig. 1. The experiments are discussed in detail in the following sections.

Free Draining (FD) Experiment

Experiment one was conducted under free draining conditions. The experiment was run for two successive irrigation events with 10 days apart. The first irrigation lasted 275 min and the second 140 min. The average inflow rates were 1.07 and 1.03 $L\cdot s^{-1}$ for the first and second irrigations, respectively. Bromide, based on $CaBr_2$ component, was injected at a constant rate during the entire first irrigation event. The average bromide concentration for the first irrigation cycle was 6.3 g $Br\cdot L^{-1}$. The second irrigation was carried out with unamended water (without bromide).

Blocked-End Experiments

Experiments two, three, and four were carried out on blocked-end furrows, using the following three solute application options (referred to further as the 100%, FH and SH experiments, respectively):

- Bromide applied during the entire irrigation event (100%);
- Bromide applied during only the first half of the irrigation event (FH); and
- Bromide applied during the second half of the irrigation event (SH).

Each of the three experiments included one irrigation, which lasted 140 min. The average inflow rates for these three runs were 1.29, 1.32, and 1.28 $L\cdot s^{-1}$, respectively. Water reached the end of the field after 107 and 114 min for the 100% and FH experiments, respectively, but did not reach the end for the SH experiment because of high roughness and high infiltration properties in that plot. Furthermore, the averaged applied bromide concentrations for the 100%, FH, and SH experiments were 2.36, 2.79, and 5.35 g $Br\cdot L^{-1}$, respectively. As indicated above, the solute application time for the 100% experiment was 140 min and 70 min for the FH and SH experiments. Relatively long solute applications were used for these experiments because of the low solute uniformity reported in the literature for borders with short application times (Playan and Faci 1997). Also, short fertilizer application times (about 10 min or so) are not common in practice. The following additional measurements were made for both the free-draining and blocked-end experiments:

- The maximum nonerosive flow rate for the field site was measured to be 1.5–1.6 $L\cdot s^{-1}$ in a pretest before performing the main experiments.
- The inflow rate was measured using 2.5-cm (1-in.) size double water meters (with two water meters on the same line). They were calibrated at the field site before being used. The inflow rate was delivered and measured at each furrow separately. Water meter readings were recorded every 5–10 min during the experiments.
- The monitored furrows were marked with stakes at 20-m intervals. Advance and recession times as well as water depth measurements were recorded at those stations along the monitored furrows. Water depths, measured using staff gauges placed at the bottom of the furrows, were initially recorded every minute for the first 10 min after advance was reached, and then every 5–10 min. They were also recorded at 2–5 min. intervals after shutting off the inflow rate until recession was complete.
- The applied bromide was metered to each experimental furrow separately using small solute boxes, each having a capacity of 4 L and equipped with valves and floaters. The bromide solution was prepared in advance in 220-L barrels. The solute boxes were then calibrated for the desired concentrations before each experiment. Later, each barrel was connected to a

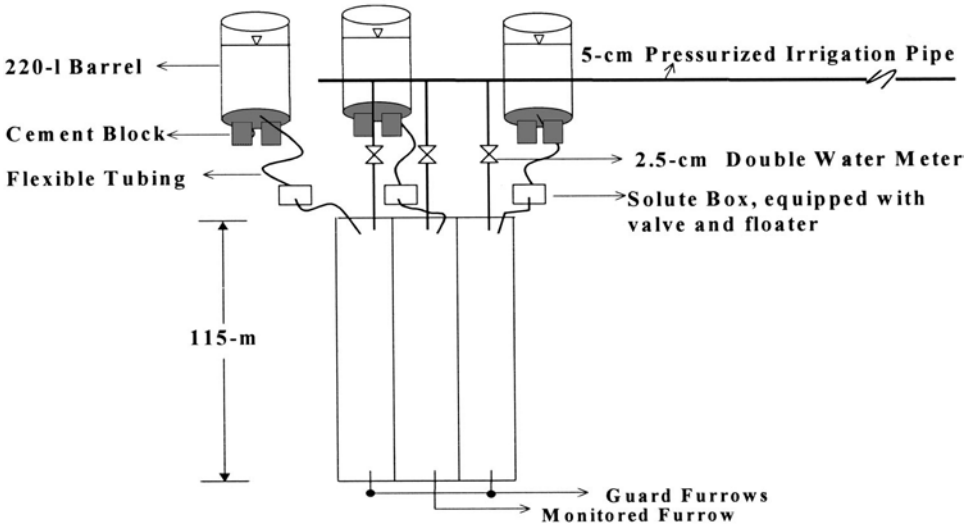

Fig. 2. Schematic of the inflow system used for the field experiments (not to scale)

solute box using 1.25-cm (1/2-in.) flexible tubing. The bromide solution was applied at the head of the furrows where the metered water was introduced (Fig. 2).

- Overland water samples for analysis of bromide concentrations were taken at three different locations—10, 60, and 100 m from the inlet for the blocked-end experiments and 5, 60, and 110 m for the free-draining experiment. Water samples at the different stations were collected as soon as water reached a particular station. Samples were initially taken at 1 min with the sampling interval increased gradually to every 10 min and then decreased to every 2–3 min after terminating the solute application (such as for the FH experiment on the blocked-end furrows). The samples were kept in an air-conditioned room and later analyzed for bromide concentrations with a Lachat QuikChem flow injection analyzer using the standard colorimetric procedure.
- Elevations of the experimental furrows were recorded using a standard surveyor's level at the stations where the water depths and advance times were recorded. The average longitudinal slope of the field was 0.0001 $m \cdot m^{-1}$ (Table 1).
- The geometry of the monitored furrows was also measured before and after the irrigation at three different locations along the monitored furrows. The average furrow cross-section (ρ_1 and ρ_2) and geometry (σ_1 and σ_2) parameters (Elliot and Walker 1982) were determined (Table 1) and later used as input to the model.
- Runoff water from the free-draining experiment was collected at the end of the furrows and pumped out using a small pump, because the furrows were almost level. The pumped water was weighed each 5 min during the irrigation time using an electrical scale.

Results and Discussion

Infiltration and Roughness Parameters

Several methods, such as ring infiltrometers, blocked furrow infiltrometers, a recirculating method, inflow-outflow method, procedures based on advance stream data, and volume balance are available for estimating infiltration parameters. The simplest method is probably the ring infiltrometer, but this method is not precise for cracking clay, freshly tilled soils, and furrows. While procedures based on advance phase data are relatively easy and simple for estimating infiltration parameters, results may not adequately represent the infiltration process during the entire irrigation cycle. Fangmeier and Ramsey (1978) found that such procedures based only on the advance phase tend to underestimate infiltration during subsequent phases of the irrigation process. Volume balance methods are usually more appropriate for determining field-scale infiltration parameters. These methods calculate the infiltrated water as the difference between the inflow volume and the volume stored on the soil surface. In this study, we used the EVALUE program developed by Strelkoff et al. (1999) to estimate the infiltration and roughness parameters for the blocked-end furrow experiments. The EVALUE estimates the infiltration parameters in a modified Kostiakov branch function, Eq. (6), by matching measured growth of infiltrated volumes to those calculated on the basis of the measured advance. The technique also generates an estimate of the roughness coefficient in the Manning formula. It assumes that water velocities are small (generally lower than 0.1 $m \cdot s^{-1}$), which is common for surface irrigation, particularly for flat fields in which case the water surface slope, $\partial y/\partial x$, can be considered equal to the friction slope, S_f. The hydraulic radius, R, is found using the measured flow depths and the either power law or trapezoidal cross section shape. Local discharges are estimated using an integrated form of the continuity equation, Eq. (4).

Infiltration and roughness parameters for the blocked-end experiments as estimated using the EVALUE program are given in Table 1. Both the estimated infiltration and roughness values were consistent between the 100% and FH experiments, whereas the infiltration coefficients k and the Manning n were substantially higher for the SH experiment. Based on field observations, we suspected higher infiltration and roughness values for the SH experiment, because with almost the same inflow rate water failed to reach the end of the field, Fig. 3(d), while it reached the end in 107 and 114 min for the 100% and FH experiments, respectively. The exponent ''a'' in Eq. (6) was found to be essentially the same for all experiments and we obtained relatively small values for the fitting of parameter ''c.'' A sensitivity analysis showed that the

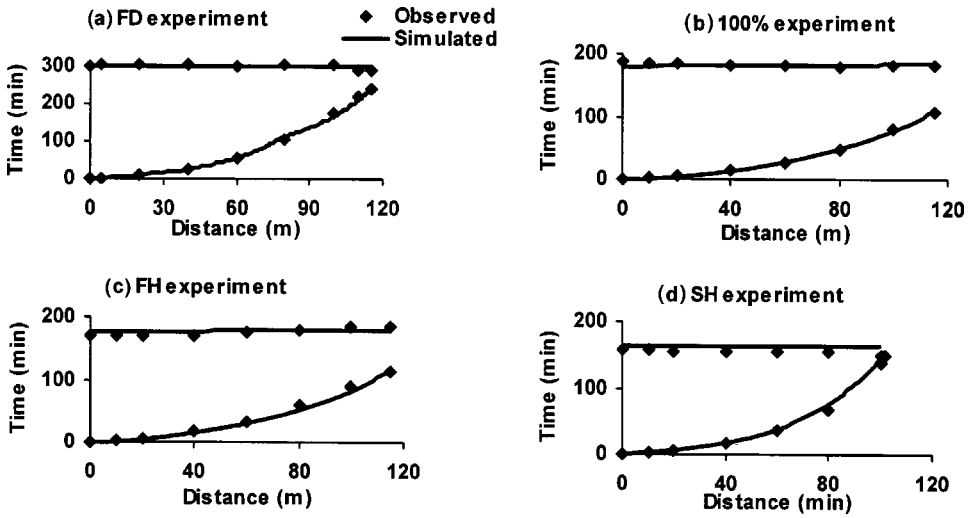

Fig. 3. Measured and simulated advance and recession times for the different field experiments: (a) free draining experiment; (b) 100% experiment; (c) first-half experiment; (d) second-half experiment

model was not sensitive to this parameter. For example, increasing "c" from 0.001 to 0.006 increased the total advance time at the end of the field by only about 2–3 min (results not shown).

The EVALUE program was specifically designed for blocked-end fields without runoff, so the infiltration parameters for the FD experiment were estimated using the following volume balance equation:

$$V_i = V_y + V_z - V_R \tag{17}$$

where $V_i\,(\mathrm{m}^3)$ = inflow volume; $V_y\,(\mathrm{m}^3)$ = stored volume on the soil surface; $V_z\,(\mathrm{m}^3)$ = infiltrated volume; and $V_R\,(\mathrm{m}^3)$ = runoff volume at the end of the field.

The stored volume on the soil surface was estimated from the measured flow depths using trapezoidal interpolation. The estimated infiltration parameters using this approach were more or less the same as those obtained for the 100% and FH experiments using the EVALUE program (Table 1). The infiltration rate did not reach a steady state (final infiltration rate) within the duration of all experiments. For this reason, we only estimated the coefficients a, k, and c for Eq. (6). The average value of the Manning n for the blocked-end experiments was taken as the roughness value for the FD experiment

Advance and Recession Trajectories

Simulated and observed water advance and recession times for all four experiments are shown in Fig. 3. In general, excellent agreement exists between the simulated and measured results for all runs in both the advance and recession phases. In a few cases, the model slightly underestimated, Fig. 3(c), or overestimated, Fig. 3(d), the advance and recession times, respectively. Likely reasons for this were spatial and temporal variability in infiltration and roughness parameters and nonuniformity of the field slope along the furrows. The water balance errors were 1.8, 1.3, 0.004, and 1.6% for the 100%, FH, SH, and FD experiments, respectively. Results were obtained using the same time increments, $\Delta t = 3$ min for all simulations.

Overland Solute Concentration

Observed and simulated overland solute concentrations at different stations along the experimental furrows are shown in Fig. 4. Some deviations in solute concentrations are apparent at the beginning of the experiments. This is due mainly to undesired inflow rate changes. Although the solutes were applied uniformly during the application time, any variation in inflow rate, which is common especially at the beginning of an irrigation event, could change the applied solute concentration. Any changes at the source point should be visible at especially the first stations close to the input source. A minor part of the concentration variations could possibly be attributed also to dispersivity. The dispersivity parameter, D_l, was found to be 10 cm using model calibration. Calibration procedure and the effects of D_l on the results are discussed in detail in the following section.

The applied solute concentration for the FD experiment Fig. 4(a) decreased from an average of 6.75 to 6 $\mathrm{g\,Br \cdot L^{-1}}$ after 110 min because of increasing inflow rate from an average of 0.97 to 1.14 $\mathrm{L \cdot s^{-1}}$. Notice that the peak values of the relative concentration at the three monitoring stations did not show any decay in time and remained more or less the same because of a relatively long application time and the short field length. The steep rise at the beginning of each break through curve (BTC) was due to the high flow velocity for the surface irrigation, as compared to flow and transport fluxes in soils, which caused concentrations reaching the maximum rate shortly after water flow arrived a given station.

From Fig. 4, we can conclude that the model simulated all experiments relatively well. The model predicted slightly longer duration of the solute peak at the third monitored stations (100 m) for the FH and SH experiments, Figs. 4(c) and 4(d), as compared to field data, most likely due to spatial variability in soil infiltration and roughness properties. The later also caused relatively poor arrival estimate of bromide to station 100-m at FH experiment, Fig. 4(c).

Dispersion Coefficient

A sensitivity analysis was carried out to assess the effects of the dispersivity, D_l in Eq. (3), on overland solute concentrations and also to estimate a reasonable value for this parameter. The model was run with three different values of D_l, 1, 10, and 100 cm. Results for the FH experiment were selected and shown in Fig. 5. Clearly, all three D_l values produced more or less the same fit with measured data at all stations. Simulated peak values of the

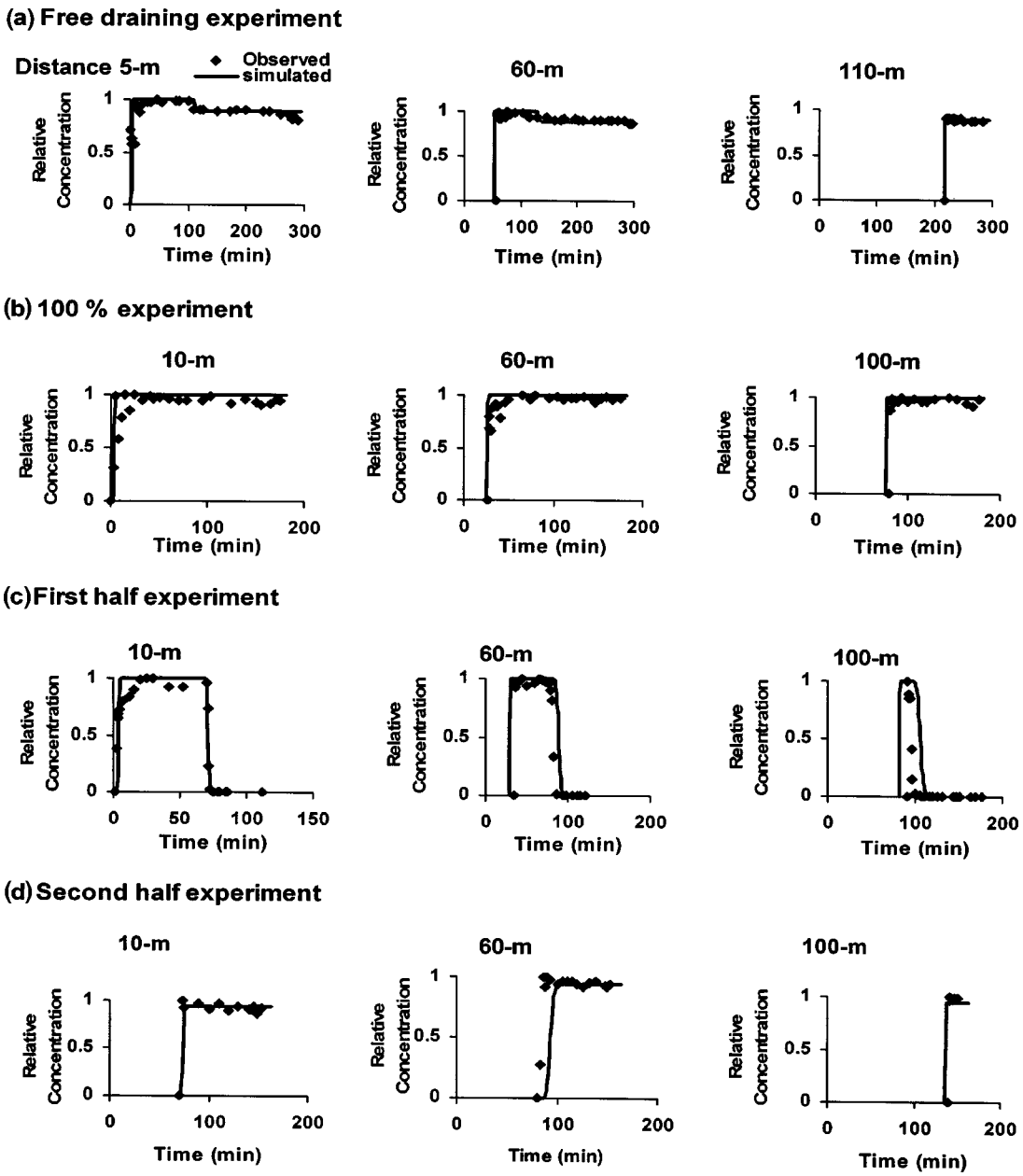

Fig. 4. Relative solute concentrations for the different experiments: (a) free draining experiment; (b) 100% experiment; (c) first-half experiment; (d) second-half experiment

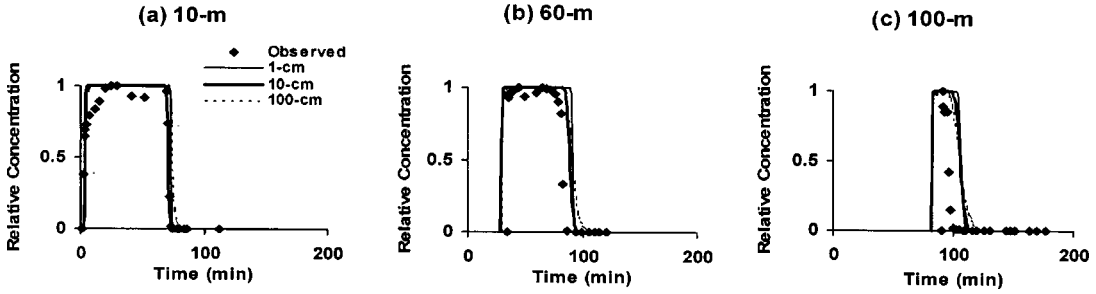

Fig. 5. Sensitivity of the overland solute concentrations to different values of the dispersivity parameter performed using the first-half experimental data: (a) 10-m station; (b) 60-m station; (c) 100-m station

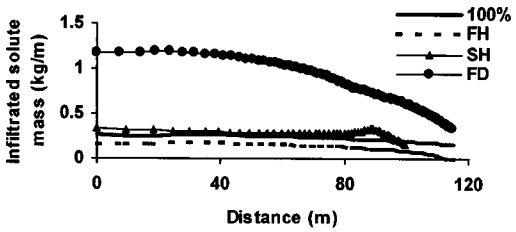

Fig. 6. Predicted infiltrated solute mass along the field for the different experiments

relative solute concentrations remained 1.0 for all monitored stations regardless of the selected D_l-value because of the minor effect of the dispersivity values on the results. A value of 10 cm was chosen for D_l in all subsequent simulations. Effect of selected D_l values on solute concentrations in other experiments (FD, 100%, and SH) was almost negligible (not shown here). The effect of dispersivity on the solute uniformity was also negligible.

Neither oscillation behavior nor numerical diffusion were found even with applying $D_l=0$ (pure advection) likely because of choosing appropriate values for the Peclet and Courant numbers. Solute BTCs remained as a rectangle, with relative solute concentration equal to 1.0, while applying $D_l=0$ [in this case Δx was assumed to be 0.5 m and Δt was determined using Eq. (14) while in other cases Δx and Δt were directly calculated from Eqs. (13) and (14)].

Assuming $D_l=10$ cm, the dispersion coefficient K_x in Eq. (3) varied between 4×10^{-8} and 0.00745 $m^2\cdot s^{-1}$ in our study. This is because K_x strongly depends upon the overland flow velocity, which varies with time and distance. In addition to a transient velocity distribution, K_x in overland studies also can be affected by shear velocity, hydraulic radius, and flow area/flow depth (Cunge et al. 1980). As indicated earlier, Garcia-Navarro et al. (2000) obtained a much larger, constant value of 0.075 $m^2\cdot s^{-1}$ for K_x by calibrating their model to their steady-state experimental data using an impervious border. Still larger K_x values are reported in the literature in hydrological studies. For instance, Brebion et al. (1971) obtained a value of 2 $m^2\cdot s^{-1}$ for K_x in the Vienne River in France. We believe that smaller obtained values for K_x in this study are more physical than the previously reported values for borders and rivers, one to several magnitudes of orders larger than physical values. Another possible reason for the discrepancy could be associated to small confined flow area (and relatively short lengths in this study) in furrows, which consequently result in almost instantaneous solute mixing, compared to wide and longer borders and particularly rivers. In fact, K_x values in both borders and rivers, resulted in 1D analysis, represent an average for the longitudinal and transverse dispersion coefficient while in furrows essentially represent longitudinal dispersion coefficient because of the indicated reason above.

Table 2. Measured and Predicted Water and Solute Distribution Uniformities of the Low Quarter, DU_{LQ}, and Low Half, DU_{LH}, for Different Field Experiments (%)

	Predicted Water		Predicted Solute		Measured Solute	
Experiment	DU_{LQ}	DU_{LH}	DU_{LQ}	DU_{LH}	DU_{LQ}	DU_{LH}
100%	77.8	85.3	77.8	85.3	75.6	87.4
First-half, FH	74.6	83.5	32.2	62.2	20.6	61.8
Second-half, SH	52.8	70.8	83.0	91.6	38.7	73.9
Free draining, FD	57.8	73.3	57.8	73.3	34.5	71.9

Infiltrated Solute Mass

The amount of infiltrated bromide along the furrows (Fig. 6) was calculated with Eq. (15) using the predicted infiltrated water depths and overland solute concentrations. The uniformity of the chemigation process was also evaluated using DU_{LQ} and DU_{LH} terms and presented in Table 2 for the different field experiments. Bromide application decreased with distance for the FD experiment, Fig. 6. In addition, both the water and solute uniformities for this experiment were lower than for the 100% and SH experiments (Table 2). These results were due mostly to the applied inflow rate and applied solute mass. Irrigation uniformity depends greatly upon the inflow rate. As stated above, the average inflow rate for the FD experiments was only 1.07 $L\cdot s^{-1}$, which is lower than for the other three experiments (about 1.3 $L\cdot s^{-1}$). Consequently, much more water (and hence solutes) infiltrated at small distances from the inlet. Furthermore, the average applied solute concentration during the first 110 min of irrigation (6.75 $g\,Br\cdot L^{-1}$) was somewhat higher than for the rest of the irrigation (6 $g\,Br\cdot L^{-1}$). An overall large amount of infiltrated bromide for the FD experiment was due to a longer (2–4 times) solute application time as compared to the other experiments.

The 100% and FH experiments provided higher irrigation DU_{LH} values while the 100% and SH experiments gave higher solute DU_{LH} values (Table 2). This means that applying the fertilizer during the entire irrigation, or during the second half of the irrigation, with an inflow rate close to the maximum nonerosive inflow rate, can provide high irrigation and fertilization uniformity. However, applying fertilizers during the entire irrigation event may cause losses of the fertilizers due to deep percolation. Applying fertilizers during the second half of the irrigation event, or even later, particularly under blocked-end conditions, could significantly reduce the solute deep percolation and increase solute uniformity. However, in the presence of runoff (i.e., free drainage), applying the solute during the second half of the irrigation will increase solute losses due to runoff from the end of field. A comparison between solute uniformities obtained in this study and those reported in the literature for borders (Playan and Faci, 1997; Garcia-Navarro et al. 2000) shows a higher solute uniformity for our furrow experiments. This may be attributed to our relatively long solute application times, as well as the inherently higher irrigation uniformity of furrows.

The agreement between measured and predicted results for the solute DU_{LH} was satisfactory, whereas the agreement for the DU_{LQ} values was not as good as DU_{LH}. The discrepancy between measured and predicted values may be attributed to the limited number of measured points used in the calculations. The measured DU_{LQ} and DU_{LH} values were calculated based on four measured points located 0, 10, 60, 100 m away from the inlet for the blocked-end experiments. The measured points for the FD experiment were located at 0, 5, 60, and 110 m from the inlet. More measurement points, probably, would have improved consistency. The model gave the same water and solute uniformities for the 100% and FD experiments, because the solutes were continuously applied with irrigation water. Low water uniformity for the SH experiment (Table 2) was due to high infiltration rate and likely also the roughness at the end of the field which resulted in water never reaching the end of the furrow. The model accounted for over 96% of the applied solute. Fertilizer mass balance errors for the 100%, FH, SH, and FD experiments were 2.2, 3.6, 2.3, and 1.2%, respectively. Moreover, measured and predicted fertilizer losses through the runoff at the end of the FD experiment were found to be 1.46 and 1.36%, respectively.

Summary and Conclusions

A combined overland water flow and solute transport model was developed and used to evaluate several alternative fertigation practices used in furrow irrigation field experiments. Contrary to the former solutions for 1D advection-dispersion equation reported in the literature in hydrological (Leendertse 1970; Brebion et al. 1971) and fertigation (Playan and Faci 1997; Garcia-Navarro et al. 2000) studies, which applied two-step schemes to avoid numerical dispersion and used Courant number as stability criteria, in the present study a Crank-Nicholson finite-difference scheme and two dimensionless numbers, Peclet and Courant numbers, were used in solving the advection-dispersion equation. The applied scheme did not show oscillation behavior and numerical dispersion most likely due to the appropriate selected values for the Peclet and Courant numbers (10 and 1, respectively).

In spite of recognized 2D water flow and solute movement in furrows, presented 1D solution of the overland water flow and transport equations adequately described and provided a reasonable picture of the intended chemigation likely due to inherent small flow areas and relatively larger surface flow velocities in furrows, which in turn reduce lateral flow and solute displacement. Both measured and predicted water and solute uniformities showed a high dependency to the inflow rates, as the upstream boundary condition, soil infiltration, and roughness properties, as well as solute application time, whereas dispersivity and concentration of the input solute had a minor influence on the fertigation uniformities.

Although the experiments were conducted adjacent to each other, estimated soil infiltration and roughness characteristics revealed some spatial variability among the monitored furrows that affected water advance and recession trajectories, and consequently the irrigation and solute uniformities. Both field measured and model predictions concluded that application of fertilizers during either the entire irrigation event or the second half of the irrigation, resulted in higher solute uniformity under blocked-end conditions. Also, a sensitivity analysis showed that the longitudinal dispersivity did not play an important role in our surface chemigation experiments, nor had a significant effect on the overland solute concentrations. This may have been partly due to relatively short experimental furrows in this study and partly due to small confined flow areas in furrow irrigation. We believe that the presented model is capable of assessing more complicated and realistic fertigation alternatives. However, more research for verifying of the obtained dispersivity parameter in longer furrows and validation of the model particularly for fertigation processes in irrigated borders are recommended.

Acknowledgments

The first writer is very grateful to Jack Jobes and JoAn Fargerlund of the U.S. Salinity Laboratory, Riverside, Calif., Carl Arterberry, Don Powers, and Candy Van Meeteren of the U.S. Water Conservation Laboratory, Phoenix, Ariz., for their help during executing the field experiments and subsequent laboratory analyses. Thanks to Robert L. Roth, director of Maricopa Agriculture Center, Phoenix, Ariz., and his colleagues for their kind collaboration during the field experiments and initial laboratory analysis. The writers also gratefully acknowledge two anonymous reviewers for their helpful comments and suggestions.

Notation

The following symbols are used in this paper:

A = cross section flow area (m^2);
a = exponent of Kostiakov branch infiltration equation (-);
b = constant in Kostiakov branch infiltration equation ($m^2 \cdot min^{-a}$);
C = solute concentration ($g \cdot L^{-1}$);
C_r = Courant number (-);
c, c_B = constants in Kostiakov branch infiltration equation ($m^3 \cdot m^{-1}$);
D_d = molecular diffusion in free water ($m^2 \cdot s^{-1}$);
D_l = longitudinal dispersivity (cm);
DU_{LH} = distribution uniformity of low half (%);
DU_{LQ} = distribution uniformity of low quarter (%);
F_R = mass of solute losses due to runoff (kg);
F_z = mass of infiltrated solute ($kg \cdot m^{-1}$);
K_x = dispersion coefficient ($m^2 \cdot s^{-1}$);
k = constant in Kostiakov branch infiltration equation ($m^2 \cdot min^{-a}$);
n = Manning's roughness ($m^{1/6}$);
P_e = Peclet number (-);
Q = flow rate ($m^3 \cdot s^{-1}$);
Q_o, Q_R = inflow and outflow rates ($m^3 \cdot s^{-1}$);
q_x = flux density ($m \cdot s^{-1}$);
R = hydraulic radius (m);
S_f, S_0 = friction and field slopes ($m \cdot m^{-1}$);
t_{co} = cut-off time (min);
U = flow velocity ($m \cdot s^{-1}$);
V_i, V_R, V_y, V_z = inflow, runoff, stored, and infiltrated volumes (m^3);
y = flow depth (m);
Z = infiltrated volume per unit length ($m^3 \cdot m^{-1}$);
Δt = time increment (min);
Δx = space increment (cm);
θ = water content ($cm^3 \cdot cm^{-3}$);
ρ_1, ρ_2 = hydraulic section parameters ($m^{3.33-2\rho_2}$,-);
σ_1, σ_2 = furrow geometric section parameters ($m^{1/2\sigma_2}$,-);
τ = infiltration opportunity time (min);
τ_B = inundation time (min); and
τ_0 = tortuosity factor(-).

References

Abbasi, F., Jolaini, M., Moaiyeri, M., Rezaee, H. T., and Shooshtari, M. M. (1999). "Development a mathematical model to evaluate and design of surface irrigation systems." *Technical Report No. 122*, Iranian Agricultural Engineering Research Institute, Karaj, Iran (in Persian).

Abbasi, F., Shooshtari, M. M., and Feyen, J. (2003). "Evaluation of the various surface irrigation numerical simulation models." *J. Irrig. Drain. Eng.*, in press.

Bear, J. (1972). *Dynamics of fluids in porous media*, Elsevier Science, New York.

Boldt, A. L., Watts, D. G., Eisenhauer, D. E., and Schepers, J. S. (1994). "Simulation of water applied nitrogen distribution under surge irrigation." *Trans. ASAE*, 37(4), 1157–1165.

Bowman, R. S., and Rice, R. C. (1986). "Transport of conservative tracers in the field under intermittent flood irrigation." *Water Resour. Res.*, 22, 1531–1536.

Brebion, S., Lebrun, B., Chevereau, G., and Preissmann, A. (1971). "Modeles mathematiques de la pollution." *IRCHA*, Centre de Recherche, 91 Vert-lepetit, France (in French).

Chow, V. (1959). *Open channel hydraulics*, McGraw-Hill, New York.

Cunge, J. A., Holly, F. M., and Verwey, A. (1980). *Practical aspects of computational river hydraulics*, Pitman, London.

Elliot, R. L., and Walker, W. R. (1982). "Field evaluation of furrow infiltration and advance functions." *Trans. ASAE*, 25(2), 396–400.

Fangmeier, D. D., and Ramsey, K. K. (1978). ''Intake characteristics of irrigation furrows.'' *Trans. ASAE,* 21, 696–700.
Garcia-Navarro, P., Playan, E., and Zapata, N. (2000). ''Solute transport modeling in overland flow applied to fertigation.'' *J. Irrig. Drain. Eng.,* 126(1), 33–40.
Hanson, B., Bowers, W., Davidoff, B., Kasapligil, D., Carvajal, A., and Bendixen, W. (1995). ''Field performance of micro-irrigation systems, Micro-irrigation for a changing word: Conserving resources/ preserving the environment.'' *Proc., 5th Int. Micro-Irrigation Congress*, 769–774.
Holley, E. R. (1971). ''Transverse mixing in rivers.'' *Report No. S132*, Delft Hydraulic Laboratory, Delft, The Netherlands.
Huyakorn, P. S., and Pinder, G. F. (1983). *Computational methods in subsurface flow*, Academic, London.
Jaynes, D. B., Bowman, R. S., and Rice, R. C. (1988). ''Transport of conservative tracers in the field under continuous flood irrigation.'' *Soil Sci. Soc. Am. J.*, 52, 618–624.
Jaynes, D. B., Rice, R. C., and Hunsaker, D. J. (1992). ''Solute transport during chemigation of a level basin.'' *Trans. ASAE,* 35(6), 1809–1815.
Leendertse, J. J. (1970). ''A water quality simulation model for well-mixed estuaries and coastal seas: Vol. I., Principles of computation.'' *Rand Corporation Memorandum, RM-6230-RC.*
Merriam, J. L., and Keller, J. (1978). *Farm irrigation system evaluation: A guide for management*, Utah State Univ., Logan, Utah.
Playan, E., and Faci, J. M. (1997). ''Border irrigation: Field experiment and a simple model.'' *Irrig. Sci.*, 17(4), 163–171.
Rice, R. C., Bowman, R. S., and Jaynes, D. B. (1986). ''Percolation of water below an irrigated field.'' *Soil Sci. Soc. Am. J.*, 50, 855–859.
Strelkoff, T. S., and Clemmens, A. J. (2000). ''Approximating wetted perimeter in a power-law cross section.'' *J. Irrig. Drain. Eng.*, 126(2), 98–109.
Strelkoff, T. S., Clemmens, A. J., El-Ansary, M., and Awad, M. (1999). ''Surface irrigation evaluation models: Application to level basin in Egypt.'' *Trans. ASAE,* 42(4), 1027–1036.
Thomas, L. H. (1949). ''Elliptic problems in linear difference equations over a network.'' *Report of Watson Science Computing Laboratory*, Columbia Univ., New York.
Threadgill, E. D. (1985). ''Chemigation via sprinkler irrigation: Current status and future development.'' *Appl. Eng. Agric.*, 1(1), 16–23.
Threadgill, E. D., Eisenhauer, D. E., Young, J. R., and Bar-Yosef, B. (1990). ''Chemigation.'' G. J. Hoffman, T. A., Howell, and K. H. Solomon (eds.) *Management of farm irrigation systems*, ASAE, St. Joseph, Mich., 747–780.